Journal of Hydrology (2007) 335, 68–77

available at www.sciencedirect.com

ScienceDirect

journal homepage: www.elsevier.com/locate/jhydrol

Forecasting solute breakthrough curves through the unsaturated zone using artificial neural networks

Heesung Yoon, Yunjung Hyun, Kang-Kun Lee *

School of Earth and Environmental Sciences (BK21 SEES), Seoul National University, Seoul 151-747, Republic of Korea

Received 21 September 2005; received in revised form 26 October 2006; accepted 2 November 2006

KEYWORDS
Unsaturated zone;
Solute breakthrough curve;
Artificial neural network;
HYDRUS-2D

Summary Effective groundwater management requires precise forecasting of the amount of contaminants intruding into groundwater from the surface. In this study, solute breakthrough curves throughout the unsaturated zone were predicted using artificial neural networks (ANNs), through numerical tests and through laboratory experiments. In the numerical tests, the applicability of the ANN model to the prediction of breakthrough curves was evaluated using synthetic data generated by a groundwater flow and transport model in a variably saturated media, HYDRUS-2D. The use of two ANNs, one for solute arrival times and the other for solute mass breakthroughs after the solute arrival time, was suggested in order to reduce the prediction error. The results showed that the network building process was essential in ANN model applications. The best ANN model gave a correlation coefficient value between target and output values of over 0.98. The sensitivity analysis of data forms for the network training demonstrated that regular breakthrough curves that contain a peak value can train the ANN model effectively. Then, the ANN model was verified using laboratory data obtained by tracer infiltration tests in a sand column. The overall results demonstrate that the ANN model can be an effective method for forecasting solute breakthrough curves through the unsaturated zone when hydraulic data are available.
© 2006 Elsevier B.V. All rights reserved.

Introduction

Groundwater begins to be polluted when surface contaminants infiltrate the unsaturated zone and reach the groundwater table. Thus the characterization of contaminant transport in the unsaturated zone is important for effective groundwater management. The unsaturated zone is often a highly heterogeneous medium with water contents varying substantially in space. There have been many attempts to describe the mechanisms of water and solute movement through unsaturated zones (Butters et al., 1989; Tseng and Jury, 1994; Simunek et al., 2002; Skaggs et al., 2004).

One of the most common approaches is to apply conventional physical models for solute transport through the unsaturated zone which are governed by the convection

* Corresponding author. Tel.: +82 2 880 8161; fax: +82 2 871 3269.
E-mail address: kklee@snu.ac.kr (K.-K. Lee).

0022-1694/$ - see front matter © 2006 Elsevier B.V. All rights reserved.
doi:10.1016/j.jhydrol.2006.11.001

dispersion equation (CDE) with several assumptions. These models use constant parameters for the CDE, which are valid only after solute mixing is complete throughout a volume of soil in which non-uniform velocities occur. Due to this limitation, there are models that are intended to be used only for the cases when either water velocity is relatively uniform or when substantial time has elapsed since the solute was introduced into the soil (Jury et al., 1991; Tseng and Jury, 1994).

Transfer functions have been used as an alternative approach (Jury, 1982; Jury and Sposito, 1986; White et al., 1986; Butters and Jury, 1989; Skaggs et al., 1998). The transfer function model initiated by Jury (1982) follows the concept of Black Box model based on a linear relationship between inputs and outputs. It represents solute transport in soil without an explicit description of the physical transport processes, using a probability density function of the solute travel time through the unsaturated zone.

Recently, the application of artificial neural networks (ANNs) as an approach to forecasting water resource variables is growing (Zealand et al., 1999; Sharma et al., 2003; Jain et al., 2004). The ANN is a flexible mathematical structure patterned after a biological nervous system and is considered the standard computational tool for nonlinear problems in a variety of fields. However, the building process of an ANN is not standardized and it is difficult to assess whether ANN results are optimal or not. Therefore it is important to discover the optimal network architecture and network parameters for a given system (Maier and Dandy, 2000). For solute transport problems, ANN applications have been used to predict the transport parameters and solute distribution in groundwater (Morshed and Kaluarachchi, 1998; Almasri and Kaluarachchi, 2005). Morshed and Kaluarachchi (1998) conducted numerical tests for the unsaturated flow and solute transport. They considered various parameters for properties of the medium and contaminant including grain size, hydraulic conductivity, dispersivity, solute sorption and decay, and the boundary condition including various water fluxes on the surface. They successfully predicted four key parameters of the breakthrough curve in typical groundwater remediation problems, which were breakthrough time, time to reach MCL, time to maximum concentration, and maximum concentrations.

In farmlands, it is necessary to spread solutes on the surface such as fertilizers and pesticides. For preventing the groundwater contamination, an optimal application method of surface contaminants including their concentration and application time should be suggested. As a preliminary work to this problem, the solute transport through the unsaturated zone under various surface boundary conditions should be predicted. Moreover, it is necessary to predict the solute transport with respect to elapsed time, both for accurate predictions of the mass of solutes reaching the groundwater table and for coupled simulations of solute transport in the unsaturated zone and groundwater. In this study, the applicability of ANN models for predicting solute transports throughout the unsaturated zone was investigated. We considered constant values of hydraulic parameters and non-reactive solute transports, which were simpler cases for the medium and contaminant than Morshed and Kaluarachchi (1998)'s. Instead we focused on predicting breakthrough curves under various boundary conditions including water flux, injected solute concentration and duration of solute injection. These considerations of boundary conditions on the surface will be useful for the management of water resources in agricultural areas. In this study, for accurate prediction of breakthrough curves, a dual ANN model was suggested in numerical tests and verified by laboratory experiments.

Artificial neural network (ANN)

In general, ANNs are composed of input, hidden and output layers, and each layer contains nodes. The basic comprehensive information on ANNs is presented in the following literatures (Hagan et al., 1996; Maier and Dandy, 1996; Mehrotra et al., 1997). For the construction of an ANN framework, a feed forward network with one hidden layer and a back propagation algorithm was used in this study.

Feed forward network

A feed forward network is one of the most common neural nets. In this network, nodes in one layer are connected to nodes in the next layer successively. Fig. 1 represents the conceptual diagram of a feed forward network. Mathematical descriptions of a feed forward process are as follows

$$s_j^J = \sum_i w_{ji}^{JI} x_i^I + b_j^J \tag{1a}$$

$$x_j^J = f_J(s_j^J) \tag{1b}$$

$$s_k^K = \sum_j w_{kj}^{KJ} x_j^J + b_k^K \tag{2a}$$

$$x_k^K = f_K(s_k^K) \tag{2b}$$

where superscripts I, J and K indicate the input, hidden and output layers, respectively, subscripts i, j and k mean the nodes of I, J and K layers, respectively, x denotes the nodal value, w denotes the weight between two nodes, b denotes the nodal bias, s denotes the weighted summation of nodal values in the previous layer with a nodal bias, and

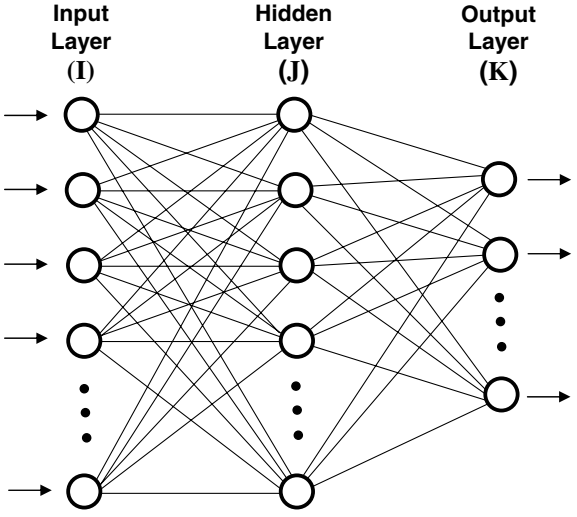

Figure 1 Conceptual diagram of a feed forward network with one hidden layer.

f is an activation function of each layer. Specific meanings of nodes in the input and output layer for this study are described in the section ''Numerical tests''. A nodal value in the hidden and output layer is determined by the activation function that transfers a weighted summation of nodal values in the previous layer. Sigmoidal-type functions are most commonly used as the activation functions (Hsu et al., 1995; ASCE Task Committee, 2000; Kuo et al., 2004). It has been also reported that using sigmoidal-type functions in the hidden layers and linear functions in the output layer can improve the extrapolation ability of the ANN (Maier and Dandy, 2000). In this study, a log-sigmoid activation function was used for the hidden layer, and a linear function was used for the output layer. Eq. (3) represents the log-sigmoid activation function used in this study

$$f(s) = \frac{1}{1 + e^{-s}} \tag{3}$$

Back propagation algorithm

The back propagation algorithm was used to determine a set of weights and nodal biases that minimize errors between target values and calculated output values after the feed forward process was completed (Rumelhart et al., 1986). For the back propagation algorithm, this study used the objective function given by the sum of squared errors between target and output values:

$$E^m = \sum_k (t_k^m - x_k^m)^2 \tag{4}$$

where E^m is the sum of squared error at the mth feed forward process, k denotes the node in the output layer, t_k^m is the target value and x_k^m is the nodal value of the output layer at the mth feed forward process. The weights, w, and nodal biases, b, in Eq. (1) are updated by the gradient descent method until the error (E) is decreased to a specific level.

$$w^{m+1} = w^m + \gamma\left(-\frac{\partial E^m}{\partial w^m}\right) \tag{5}$$

$$b^{m+1} = b^m + \gamma\left(-\frac{\partial E^m}{\partial b^m}\right) \tag{6}$$

where w^m is the weight that is updated at mth iteration, b^m is the nodal bias at mth iteration and γ is the learning rate. The back propagation algorithm based on the gradient descent method leads weights in a neural network to a local minimum of the objective function defined in Eq. (4). In this study, a momentum term was added to Eqs. (5) and (6) to prevent the network from some local minima. This reads

$$w^{m+1} - w^m = \beta(w^m - w^{m-1}) + (1-\beta)\gamma\left(-\frac{\partial E^m}{\partial w^m}\right) \tag{7}$$

$$b^{m+1} - b^m = \beta(b^m - b^{m-1}) + (1-\beta)\gamma\left(-\frac{\partial E^m}{\partial b^m}\right) \tag{8}$$

where β is the momentum value. The momentum has an averaging effect, and diminishes the drastic fluctuation in weight changes over consecutive iterations (Rumelhart et al., 1986).

Numerical tests

Numerical tests were conducted to assess the applicability of ANN to predicting the breakthrough mass of solute. For numerical tests, a 300 cm high vertical hypothetical sand profile was considered in this study. The top boundary of the domain was established as a constant flux boundary and the bottom was established as a seepage boundary. For solute breakthrough data, solute transport was simulated using HYDRUS-2D, a finite element model for simulating groundwater flow and solute transport in variably saturated media (Simunek et al., 1996). In these numerical tests, results of HYDRUS-2D simulations composed target values, and estimations of ANN models output values. In this study, a non-reactive solute and no adsorption were assumed. Thus the decay terms were not considered and the retardation factor was equal to unity [1]. Model parameter values used in this study are presented in Table 1. We conducted 116 simulations under various boundary conditions and considered solute mass of 41 discrete times at the bottom boundary from each simulation. The solute mass was calculated using averaged solute mass flux at the bottom boundary. Thus a total of 4756 solute mass data were obtained (Table 2). The data were normalized by the total solute mass that had been injected onto the surface. For ANN applications, input variables included water flux, solute injection time, injected solute concentration onto the top boundary and elapsed time after the solute injection. The normalized solute mass at the bottom boundary was used as an output variable. The applications of ANN were undertaken at three stages: training, testing and prediction. Accordingly, the data were divided into three sets: one for each stage. Table 2 represents the arrangement of data sets.

Three numerical tests were performed in this study. In Test 1, ANN applicability was investigated using a simple network. In Test 2, the use of two networks was suggested for better prediction results. Then effects of training data forms on prediction efficiency were investigated in Test 3.

Test 1

In Test 1, we established an ANN model with four input nodes, one hidden layer and one output node. The input nodes included water flux, solute injection time, injected solute concentration and elapsed time after solute had been injected, and the output node included the solute mass at the bottom boundary after the solute had been injected on the top boundary. Fig. 2a represents a schematic dia-

Table 1 HYDRUS-2D model parameters for generation of breakthrough curves used in numerical tests

Porosity	0.43
Hydraulic conductivity	712.8 (cm/day)
α[a]	0.145 (cm)
n[a]	2.68
Dispersivity	10.0 (cm)
Retardation factor	1.0

[a] van Genuchten parameters.

Table 2 Data sets used for ANN applications in numerical tests and the range of input variables for each data set

	Training data set	Testing data set	Prediction data set	Total
Number of simulations	64	22	30	116
Number of data	2624	902	1230	4756
Range of input variables				
Water flux (cm/day)	2.0—5.0	1.0—6.0	1.0—7.2	1.0—7.2
Solute injection time (day)	0.5—2.0	0.2—3.0	0.2—3.5	0.2—3.5
Solute concentration (mg/cm^3)	0.5—3.0	0.3—4.0	0.3—5.0	0.3—5.0
Elapsed time (day)	0—60	0—60	0—60	0—60

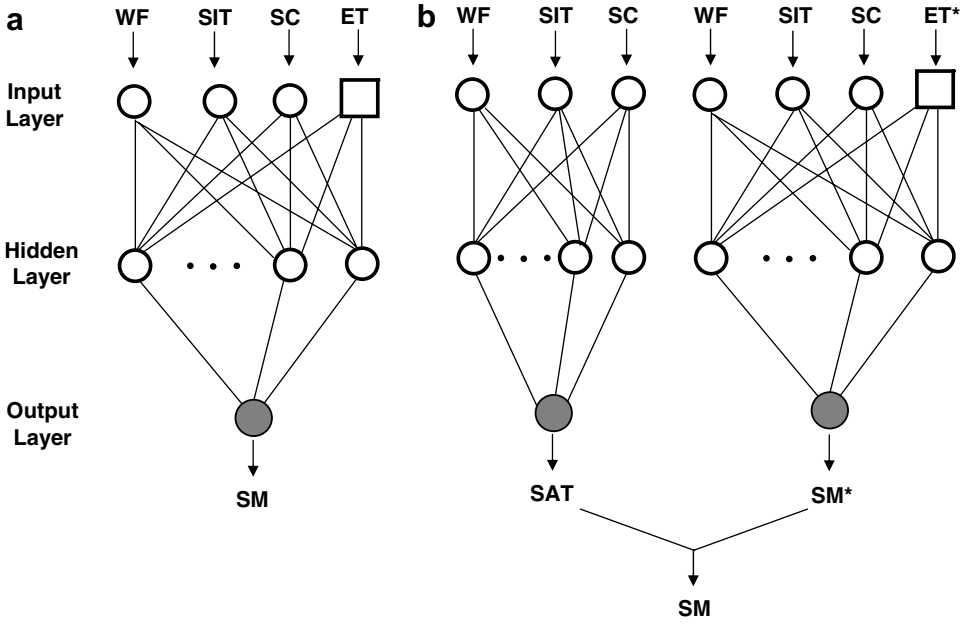

Figure 2 Schematic diagrams of the ANNs used in Test 1 (a) and Test 2 (b) (WF: water flux, SIT: solute injection time, SC: injected solute concentration, ET: elapsed time after solute injection, SM: solute mass breakthrough at the bottom with ET, ET*: elapsed time after the solute arrival at the bottom and SM*: solute mass breakthrough at the bottom with ET*).

gram of the ANN model used in Test 1. At the training stage, the weights of the ANN were calculated by the back propagation algorithm. Then the network structure and parameter values were calibrated at the testing stage by minimizing root mean square errors (RMSE) between the target and output values, given by

$$\mathrm{RMSE} = \sqrt{\frac{1}{l}\sum_m \sum_k (t_k^m - x_k^m)^2} \tag{9}$$

where l is the total number of data. The network structure included the number of hidden nodes, and the network parameters included the momentum, learning rate, range of initial weights and stopping criterion. Fig. 3 shows the RMSE values at the testing stage for various network structures and parameter values. It demonstrates that a network building process is essential in ANN applications. However, the back propagation algorithm based on the gradient descent method can seek the local minimum of any given objective function. To prevent a solution from being captured at a certain local minimum, we used the momentum and considered various initial weights. However, it can not be confirmed that the solution is the global minimum. Thus the calibrated network structure and parameter values can be the optimum only in this particular network building strategy. In Test 1, the selected number of hidden nodes was 7, momentum value was 0.4, learning rate was 0.005, range of initial weights was from -0.45 to 0.45 and stopping criterion was 4.0×10^{-3}.

The performance of the ANN was evaluated in the prediction stage. The RMSE and correlation coefficient (CC) between target and output values were calculated as prediction efficiency criteria. The CC is given by

$$\mathrm{CC} = \frac{\frac{1}{l}\sum_m \sum_k (t_k^m - \bar{t})(x_k^m - \bar{x})}{\sqrt{\frac{1}{l}\sum_m \sum_k (t_k^m - \bar{t})^2}\sqrt{\frac{1}{l}\sum_m \sum_k (x_k^m - \bar{x})^2}} \tag{10}$$

where $\bar{t}$ and $\bar{x}$ denote the mean values of the target and output values, respectively. Fig. 4 and Table 3 depict the prediction results in Test 1, and Fig. 5 shows examples of predicted breakthrough curves. The results show a good agreement between target and output values when the

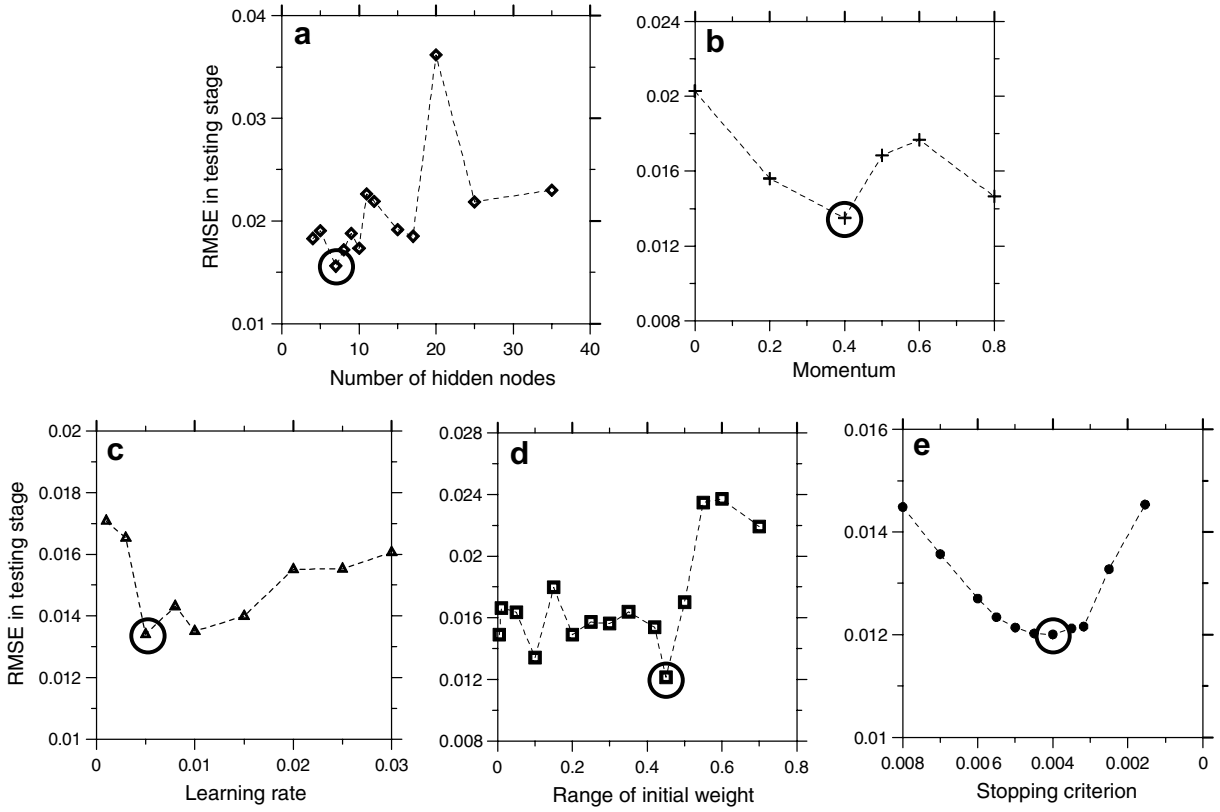

Figure 3 RMSE values in testing stage of Test 1 for various network structures and parameters: (a) number of hidden nodes, (b) momentum, (c) learning rate, (d) range of initial weights whose range is $-w_0 \sim w_0$ and (e) stopping criterion.

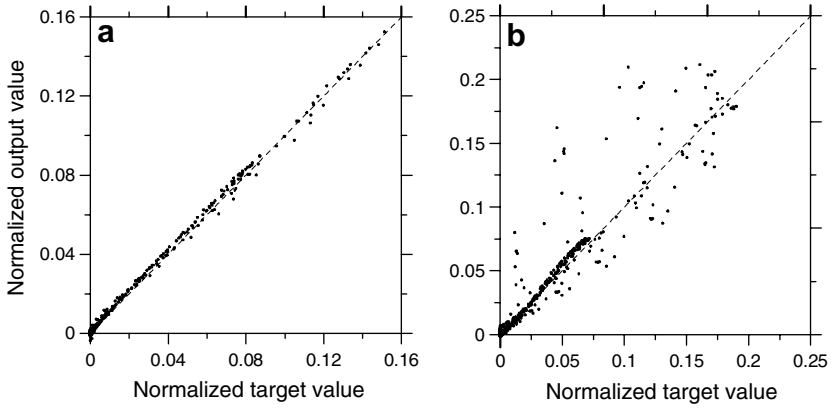

Figure 4 Correlations between target and calculated output values in Test 1 obtained from (a) inputs within the range of training data set, that include 410 data, and (b) inputs out of the range of training data set, that include 820 data, respectively.

Table 3 ANN prediction efficiencies for each numerical test

	Test 1			Test 2			Test 3		
Prediction efficiency	Within the TR. range	Out of the TR. range	Total range	SAT—ANN	SM—ANN	Combined ANN	Mass	Cumulative mass	Logarithmic mass
RMSE	1.88×10^{-3}	1.73×10^{-2}	1.41×10^{-2}	9.71×10^{-2}	7.23×10^{-3}	7.07×10^{-3}	7.24×10^{-3}	9.48×10^{-3}	1.89×10^{-1}
CC	0.999	0.930	0.946	0.998	0.983	0.983	0.983	0.980	0.891

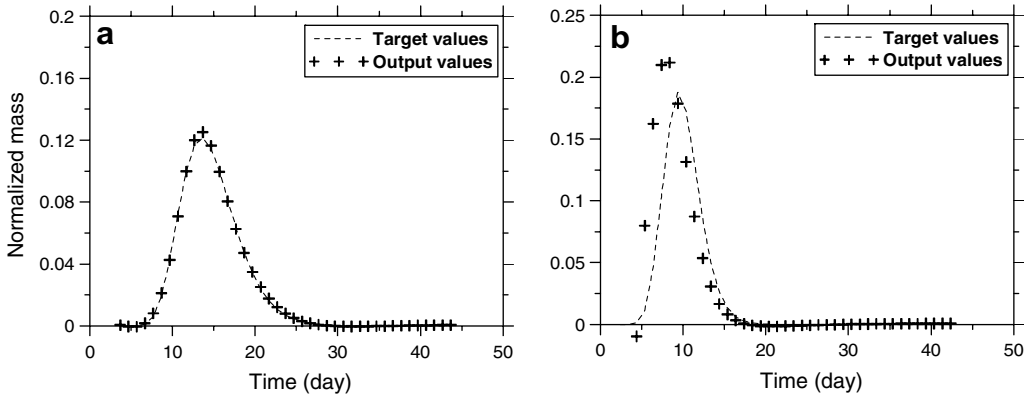

Figure 5 Examples of breakthrough curves of normalized mass predicted in Test 1: (a) the best prediction result (*CC* = 0.99) and (b) the worst prediction result (*CC* = 0.83).

input values were within the range of training data set (Figs. 4a and 5a). When the input values were out of the range of the training data set, however, the prediction efficiency was reduced considerably (Figs. 4b and 5b). In general, ANN has difficulties in extrapolating beyond the range of the data used for training (Flood and Kartam, 1994; Minns and Hall, 1996). However, it should be noted that there were large deviations near the early stages of breakthrough in most cases with input values out of the range of the training data set.

Test 2

To reduce the prediction errors observed in the early stages of breakthrough curves in Test 1, a different ANN approach was designed in Test 2. In this approach, the solute breakthrough curve was divided into two parts, one was a solute arrival time, that was an elapsed time before the solute was detected at the bottom and the other was a solute breakthrough after the solute arrival time. Thus, two ANNs were used for each part and the data sets were rearranged. Fig. 2b shows the schematic diagram of the dual ANN used in Test 2. The dual ANN model includes a network for the solute arrival time (SAT—ANN) and a network for the solute mass breakthrough after the solute arrival time (SM—ANN). SAT—ANN was composed of three input nodes, one hidden layer and one output node. The input variables were water flux, solute injection time and solute concentration. The output variable was the solute arrival time at each input event. SM—ANN was composed of four input nodes, one hidden layer and one output node. The input variables were water flux, solute injection time, solute concentration and elapsed time after the solute arrival time. The output variable was solute mass with respect to the elapsed time after the solute arrival time. SAT—ANN and SM—ANN were trained and tested separately. Then, the results were combined for the prediction of complete breakthrough curves.

Fig. 6 and Table 3 show the prediction results of ANNs in Test 2. By comparison with the results of Test 1, the prediction errors were reduced significantly for input data both within and out of the range of a training data set. Fig. 7 shows examples of predicted breakthrough curves in Test 2 under same input events as in Test 1. Notice that there were no large errors at the early stages of the breakthrough curves. These results show that predictions of solute transport using both SAT—ANN and SM—ANN were more effective than the one ANN in Test 1. Although the training

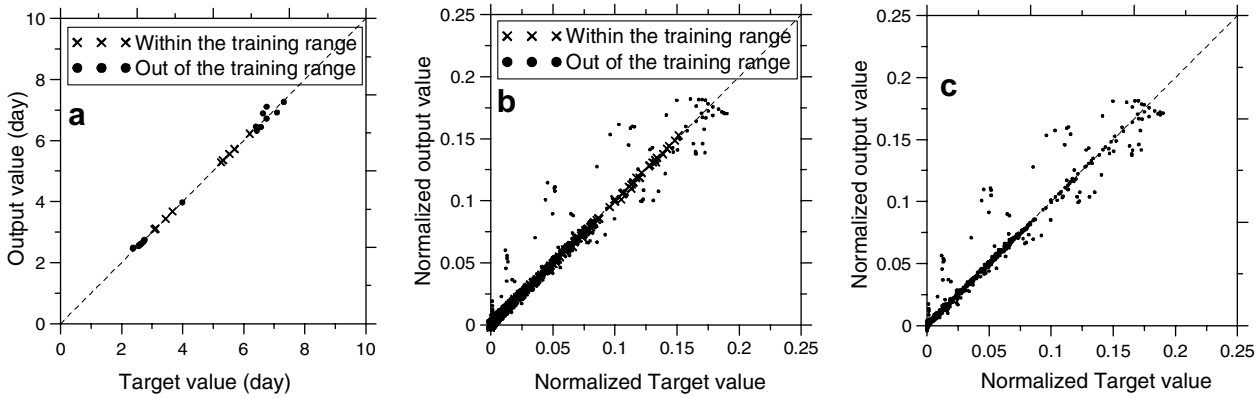

Figure 6 Correlations between target and output values of normalized mass using (a) SAT—ANN, (b) SM—ANN, and (c) combined ANN.

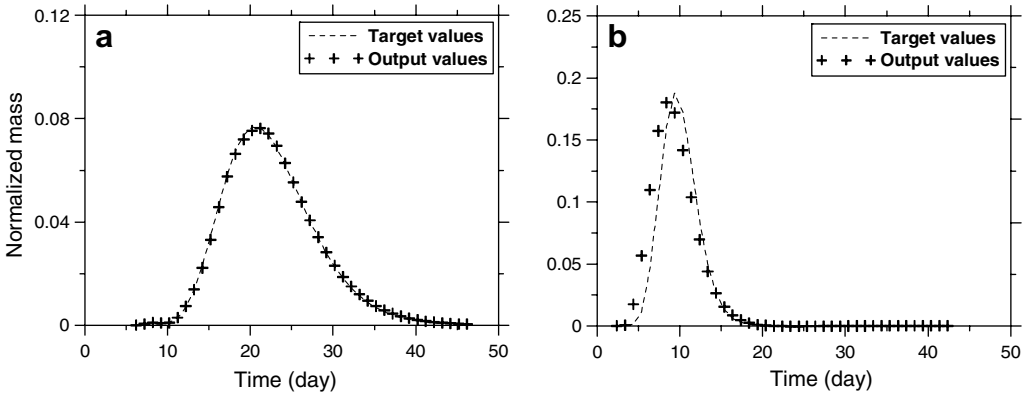

Figure 7 Examples of breakthrough curves of normalized mass predicted in Test 2: (a) the best prediction result (*CC* = 0.99) and (b) the worst prediction result (*CC* = 0.95).

procedures are more time-consuming in Test 2 than in Test 1, the network size of SAT—ANN was small and could be trained quickly and thus the total training times were comparable with Test 1.

Test 3

The ANN model is based on a data driven process, thus training data forms can affect the model efficiency. In Test 3, the influence of solute data forms on prediction efficiency was investigated using the SM—ANN in Test 2. The ANN was trained with three types of solute data; mass, cumulative mass and logarithmic mass. The data used were normalized by the total mass. Each type of data represents different curve types; peak type curves for mass data, s-shape curves for cumulative mass data and gentle slope curves for logarithmic mass data. The optimal network structures and parameters were selected for each type of data. Prediction results were compared in Fig. 8 and Table 3. When the mass data were used, ANN prediction efficiency was best. The use of cumulative mass data was likely to yield results that were overestimates and logarithmic mass data results that were underestimates. This result shows that normal peak type breakthrough curves of mass or concentration can be trained effectively and yield good prediction results for ANN applications.

Application to laboratory data

Laboratory experiments

For applications of the ANN model to laboratory experimental data, tracer infiltration tests were conducted with a sand column. The diameter and height of the sand column were 5.4 cm and 25 cm, respectively. A gravel layer of 2 cm thickness was packed at the bottom of the column for a free drainage through an output port. Then, coarse sand with grains of 0.5 mm—1.0 mm diameter was packed above the gravel layer. The porosity was 0.45. The dry and wet bulk densities were 1.65 g/cm^3 and 2.10 g/cm^3, respectively. The saturated hydraulic conductivity was estimated to be 9014.4 cm/day. The top was exposed to the air and the bottom was composed of a thin gravel layer and outlet for leaching water and tracer. Water and tracer were injected at the center of the top soil using a peristaltic pump. Br^- in KBr solution was used as a tracer. The concentration of injected solution was 2.0 g/L. The concentration of Br^- at the bottom was measured by a bromide electrode (The Thermo Orion Model 9635 ionplus). Column tests were conducted 14 times, for various water fluxes and durations of solute injection. The initial water content ranged from 0.14 to 0.15. The Br^- concentration of the leaching water was measured for each test.

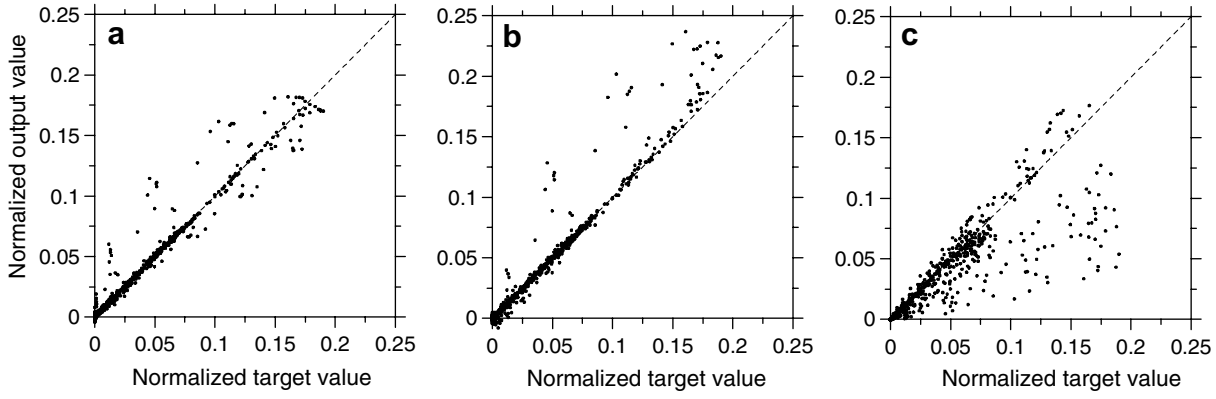

Figure 8 ANN prediction results for three forms of solute mass data: (a) mass, (b) cumulative mass, and (c) logarithmic mass.

Table 4 Data sets used for ANN application to laboratory experiments and the range of input variables for each data set

	Training data set	Testing data set	Prediction data set	Total
Column test frequency	9	2	3	14
Number of data	243	49	80	372
Range of input variables				
Water flux (cm^3/min)	2.0—6.0	3.0—5.0	2.0—7.0	3.0—7.0
Solute injection time (min)	1.0—4.0	1.5—2.0	1.0—5.0	1.5—5.0
Elapsed time (min)	0.0—191.2	0.0—114.2	0.0—191.2	0.0—172.8

ANN application

The dual ANN model used in Test 2 was applied to the experimental data in order to predict the tracer arrival time and tracer concentration. The column test data were divided into three data sets for the training, testing and prediction stages of the ANN model (Table 4). The prediction data set was composed of three input events: the input values in the two events were within the range of the training data set (water fluxes were 3.0 and 5.0 mL/min, and solute injection times were 3.0 and 1.5 min) and the other was out of the range (water flux was 7.0 mL/min and solute injection time was 5.0 min). Table 5 and Fig. 9 show the results of the ANN model predictions for the laboratory experiments. There was a good agreement between the target and output values of the tracer concentration especially when the input values were within the range of the training data set. CC values were over 0.97. The prediction efficiency was reduced, however, when the input values were out of the range of the training data set. CC value decreased to 0.64. This result demonstrates that the range of the training data set can affect the prediction efficiency considerably. Figure 10 demonstrates the comparison of breakthrough curves of between the laboratory experiment and ANN model prediction.

Table 5 ANN prediction efficiencies for laboratory experiments

Prediction Efficiency	Within the training range	Out of the training range	Total range
RMSE	2.12×10^{-2}	2.87×10^{-1}	1.64×10^{-1}
CC	0.970	0.635	0.722

Conclusions

The following conclusions can be drawn from this study.

1. The ANN network structure and parameters strongly affected the prediction efficiency. Therefore, the network building process is an essential element in ANN applications for a given problem.
2. An ANN model with a single network cannot predict solute breakthrough curves effectively especially in the early stages of their development. This study has demonstrated that an ANN model with two networks, one for solute arrival time and the other for solute breakthrough, can reduce large errors in the early part of the breakthrough curves and raise the prediction efficiency.
3. This study tested whether or not the form of the training data significantly affects the efficiency of ANN. Training data in the forms of mass, cumulative mass and logarithmic mass data were compared with each other.

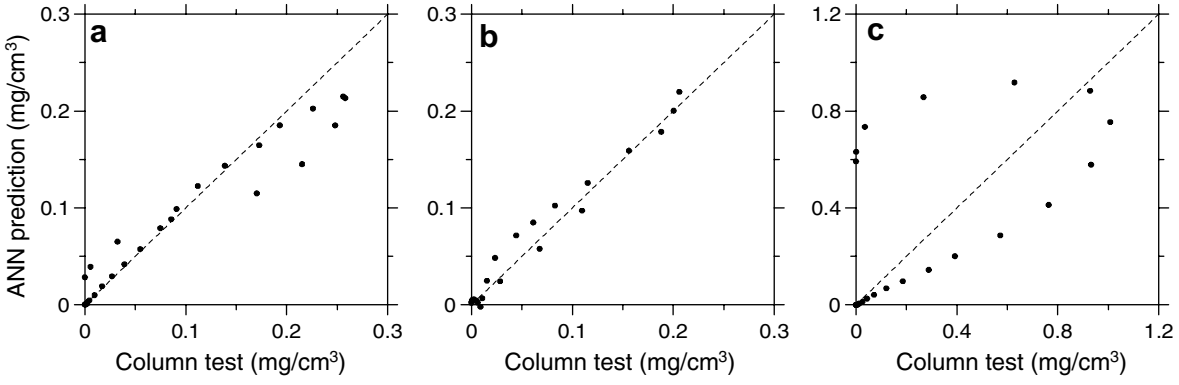

Figure 9 Comparisons of ANN prediction and experimental results of tracer concentrations: (a) WF was 3.0 cm^3/min and SIT was 3.0 min (CC = 0.98), (b) WF was 5.0 cm^3/min and SIT was 1.5 min (CC = 0.98), and (c) WF was 7.0 cm^3/min and SIT was 5.0 min (CC = 0.64).

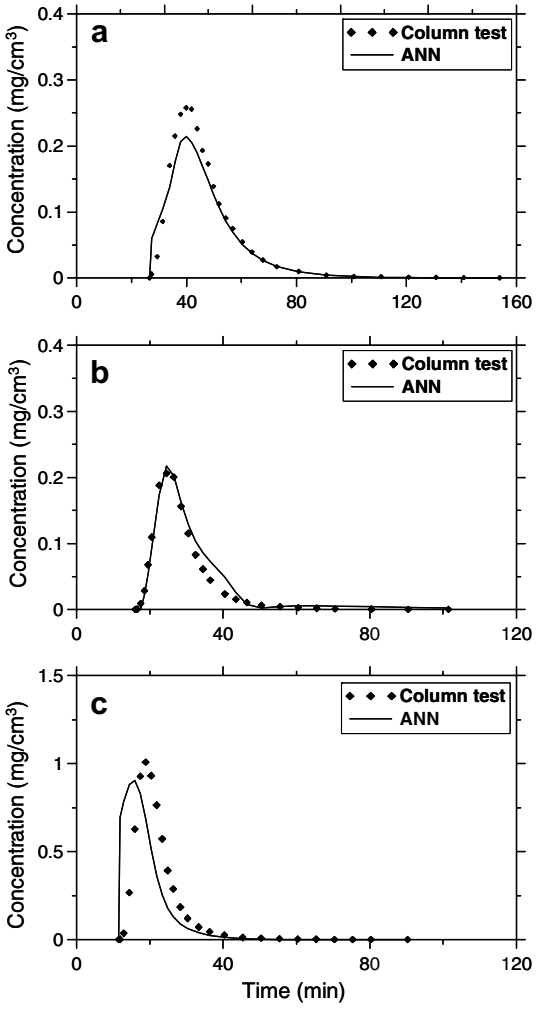

Figure 10 Comparisons of results between column tests and ANN applications: (a) WF was 3.0 mL/min and SIT was 3.0 min, (b) WF was 5.0 mL/min and SIT was 1.5 min, and (c) WF was 7.0 mL/min and SIT was 5.0 min.

The mass data associated with peak-type breakthrough curves can be trained effectively and yield good prediction results.

4. The ANN application to laboratory experimental data produced acceptable prediction results, especially when the input values were within the training data set, although the experiment frequency was limited.

Acknowledgements

This study was supported by the Advanced Environmental Biotechnology Research Center (AEBRC) at POSTECH and the Korea Energy Management Corporation (KEMCO) through KIGAM, BK21 SEES, and the Sustainable Water Resources Research Center (Project #3-4-2).

References

Almasri, M.N., Kaluarachchi, J.J., 2005. Modular neural networks to predict the nitrate distribution in ground water using the on-ground nitrogen loading and recharge data. Environmental Modelling and Software 20, 851–871.

ASCE Task Committee on Application of Artificial Neural Networks in Hydrology, 2000. Artificial neural networks in hydrology I. Preliminary concepts, Journal of Hydrologic Engineering 5, 115–123.

Butters, G.L., Jury, W.A., 1989. Field scale transport of bromide in an unsaturated soil, 2. Dispersion modeling. Water Resources Research 25, 1583–1589.

Butters, G.L., Jury, W.A., Ernst, F.F., 1989. Field scale transport of bromide in an unsaturated soil, 1. Experimental methodology and results. Water Resource Research 25, 1575–1581.

Flood, I., Kartam, N., 1994. Neural networks in civil engineering. I: Principles and understanding. Journal of Computing in Civil Engineering 8, 131–148.

Hagan, M.T., Demuth, H.B., Beale, M., 1996. Neural Network Design. PWS Publishing Company, Boston, MA.

Hsu, K., Gupta, H.V., Sorooshian, S., 1995. Artificial neural network modeling of the rainfall-runoff process. Water Resources Research 31, 2517–2530.

Jain, S.K., Singh, V.P., Barton, A.K., van Genuchten, M.Th., 2004. Analysis of soil water retention data using artificial neural networks. Journal of Hydrologic Engineering 9, 415–420.

Jury, W.A., 1982. Simulation of solute transport using transfer function model. Water Resources Research 18, 363–368.

Jury, W.A., Sposito, G., 1986. A transfer function of solute transport through soil 1. Fundamental concepts. Water Resources Research 22, 243–247.

Jury, W.A., Gardner, W.R., Gardner, W.H., 1991. Soil Physics, fifth ed. John Wiley and Sons Inc, New York.

Kuo, Y., Liu, C., Lin, K., 2004. Evaluation of the ability of an artificial neural network model to assess the variation of groundwater quality in an area of blackfoot disease in Taiwan. Water Research 38, 148–158.

Maier, H.R., Dandy, G.C., 1996. The use of artificial neural networks for the prediction of water quality parameters. Water Resources Research 32, 1013–1022.

Maier, H.R., Dandy, G.C., 2000. Neural networks for the prediction and forecasting of water resources variables: a review of modeling issues and applications. Environmental Modeling and Software 15, 101–124.

Mehrotra, K., Mohan, C.K., Ranka, S., 1997. Elements of Artificial Neural Networks. The MIT Press, Boston, MA.

Minns, A.W., Hall, M.J., 1996. Artificial neural networks as rainfall-runoff models. Hydrological Sciences Journal 41, 399–417.

Morshed, J., Kaluarachchi, J.J., 1998. Application of artificial neural network and genetic algorithm in flow and transport simulations. Advances in Water Resources 22, 145–158.

Rumelhart, D.E., McClelland, J.L.The PDP Research Group, 1986. Parallel Distributed Processing: Explorations in the Microstructure of Cognition. The MIT Press, Cambridge, MA.

Sharma, V., Negi, S.C., Rudra, R.P., Yang, S., 2003. Neural networks for predicting nitrate–nitrogen in drainage water. Agricultural Water Management 63, 169–183.

Simunek, J., Sejna, M., van Genuchten, M.Th., 1996. HYDRUS-2D, Simulating water flow and solute transport in two-dimensional variably saturated media (version 1.0), IGWMC, Golden, CO.

Simunek, J., Jarvis, N.J., van Genuchten, M.Th., Gardenas, A., 2002. Review and comparison of models for describing non-equilibrium and preferential flow and transport in the vadose zone. Journal of Hydrology 272, 14–35.

Skaggs, T.H., Kabala, Z.J., Jury, W.A., 1998. Deconvolution of a nonparametric transfer function for solute transport in soils. Journal of Hydrology 207, 170–178.

Skaggs, T.H., Trout, T.J., Simunek, J., Shouse, P.J., 2004. Comparison of HYDRUS-2D simulations of drip irrigation with experimental observations. Journal of Irrigation and Drainage Engineering 130, 304–310.

Tseng, P.H., Jury, W.A., 1994. Comparison of transfer function and deterministic modeling of area-averaged solute transport in a heterogeneous field. Water Resources Research 30, 2051—2063.

White, R.E., Dyson, J.S., Haigh, R.A., Jury, W.A., 1986. A transfer function model of solute transport through soil 2. Illustrative applications. Water Resources Research 22, 248—254.

Zealand, C.M., Burn, D.H., Simonovic, S.P., 1999. Short term streamflow forecasting using artificial neural networks. Journal of Hydrology 214, 32—48.